

## ELECTRONIC STRUCTURE AND X-RAY SPECTROSCOPIC PROPERTIES OF THE $\text{HfFe}_2\text{Si}_2$ COMPOUND

I. D. Shcherba<sup>1</sup>, V. N. Antonov<sup>2</sup>, O. V. Zhak<sup>1</sup>, L. V. Bekenov<sup>2</sup>, M. V. Kovalska<sup>1</sup>,  
H. Noga<sup>3</sup>, D. Uskokovic<sup>4</sup>, B. M. Yatcyk<sup>5</sup>

<sup>1</sup>Ivan Franko National University of Lviv, 6/8, Kyryla i Mefodiya St., Lviv, UA-79005, Ukraine

<sup>2</sup>Institute of Metal Physics, NASU, 36, Vernadskyj St., Kyiv, UA-03142, Ukraine

<sup>3</sup>Institute of Technology, Pedagogical University, 2, Podchoranzych St., Krakow, 30084, Poland

<sup>4</sup>Institute of Technical Sciences of SASA, 35/IV, Knez Mihailova, Belgrade, PO Box 37711000, Serbia

<sup>5</sup>Lviv National University of Veterinary Medicine and Biotechnologies, Ukraine

E-mail: ishcherba@gmail.com

(Received October 27, 2018; in final form — December 17, 2018)

The valence band electronic structure of  $\text{HfFe}_2\text{Si}_2$  has been established for the first time based on X-ray emission spectroscopy measurements. The band structure and X-ray emission spectra have been also obtained theoretically using the ab initio LMTO method in the non-relativistic approximation. The electron configuration of Si in the compound  $\text{HfFe}_2\text{Si}_2$  can be described as  $s^{1.1}p^{1.5}$ . The theoretical and experimental results are in satisfactory agreement.

**Key words:** X-ray spectroscopy, electronic structure, hafnium, iron.

DOI: <https://doi.org/10.30970/jps.23.2301>

PACS number(s): 32.30.-r, 71.20.Be

### I. INTRODUCTION

The  $\text{HfFe}_2\text{Si}_2$  ternary intermetallic compound [1] has a crystal structure of its own  $\text{HfFe}_2\text{Si}_2$  structure type that belongs to a large family of  $RM_2\text{Si}_2$  silicides, ( $R$  is a rare-earth element,  $M$  is Fe, Co, Ni or Cu) with  $\text{CeGa}_2\text{Al}_2$  derivative structures [2,3]. The same crystal structure occurs in the ternary silicide of iron and scandium  $\text{ScFe}_2\text{Si}_2$  as reported in Ref. [4]. The crystal structure and coordination polyhedrons of the atoms in  $\text{HfFe}_2\text{Si}_2$  are shown in Fig. 1. In this type of crystal lattice, the polyhedrons of Fe atoms have the same quantitative and qualitative composition but are different in structure. The nearest coordination environment of the atoms was described

as pseudo Frank–Kasper polyhedrons with the different numbers of the vertices: 18 vertices for  $\text{Hf}[\text{Si}_8\text{Fe}_8\text{Hf}_2]$ , 13 vertices for Fe1 and Fe2 [ $\text{Si}_5\text{Fe}_4\text{Hf}_4$ ], 11 vertices for Si1 and Si2 [ $\text{Fe}_5\text{Si}_2\text{Hf}_4$ ]. The coordination polyhedrons of the Fe atoms in this structure are the same as the polyhedrons of the Fe atoms in the structure of the binary silicide  $\text{FeSi}$ , while the polyhedrons of the Si atoms can be considered as defective icosahedra without a vertex [1]. The Fe2 atoms form lines parallel to the  $z$ -axis with a small Fe–Fe distance equal to 0.2529 nm, i.e. the same distance as in  $\alpha\text{-Fe}$  (Fig. 1, b) [2]. The Fe1 atoms contact only with Si2 atoms forming chains of quadrangles parallel to the  $y$ -axis.

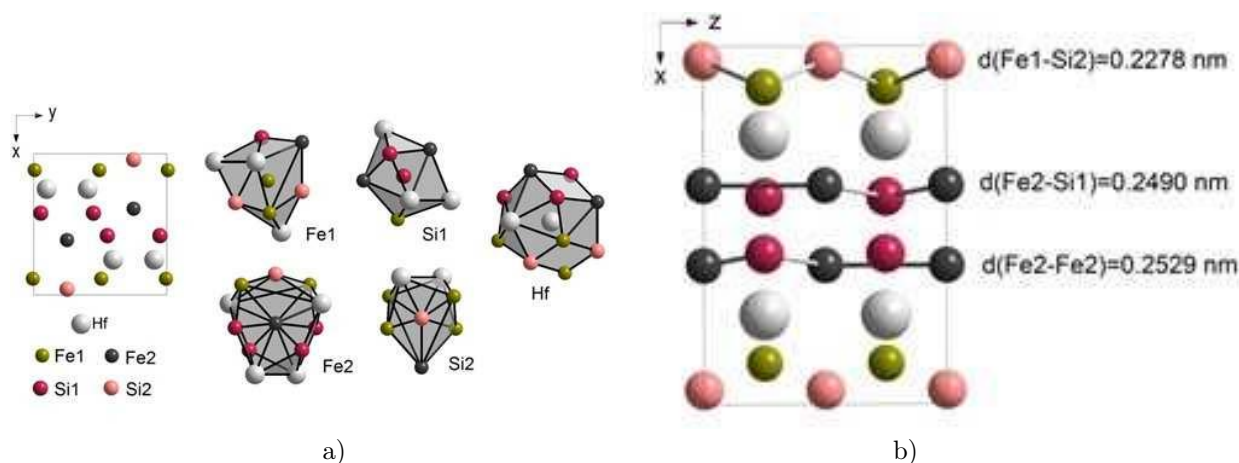


Fig. 1. XY (a) and XZ (b)-projections of the  $\text{HfFe}_2\text{Si}_2$  crystal structure and coordination polyhedrons of the atoms. The shortest interatomic distances are marked.

In the  $\text{HfFe}_2\text{Si}_2$  structure flat distorted Hf-centered hexagonal nets are formed by the Fe1 and Si1 atoms at  $z = \frac{1}{4}$  and  $z = \frac{3}{4}$  as shown in Fig. 2. The shortest interatomic distance is observed between the Fe1 and Si1 atoms, and it is equal to 0.2296 nm. The other distances are much larger, namely  $d(\text{Si1-Si1}) = 0.3722$  nm and

$d(\text{Fe1-Fe1}) = 0.3919$  nm. The Fe2 and Si2 atoms form flat distorted hexagonal nets at  $z = 0$  and  $z = \frac{1}{2}$  with the shortest interatomic distance  $d(\text{Fe2-Si2}) = 0.2594$  nm and larger ones  $d(\text{Si2-Si2}) = 0.3578$  nm, and  $d(\text{Fe2-Fe2}) = 0.3896$  nm.

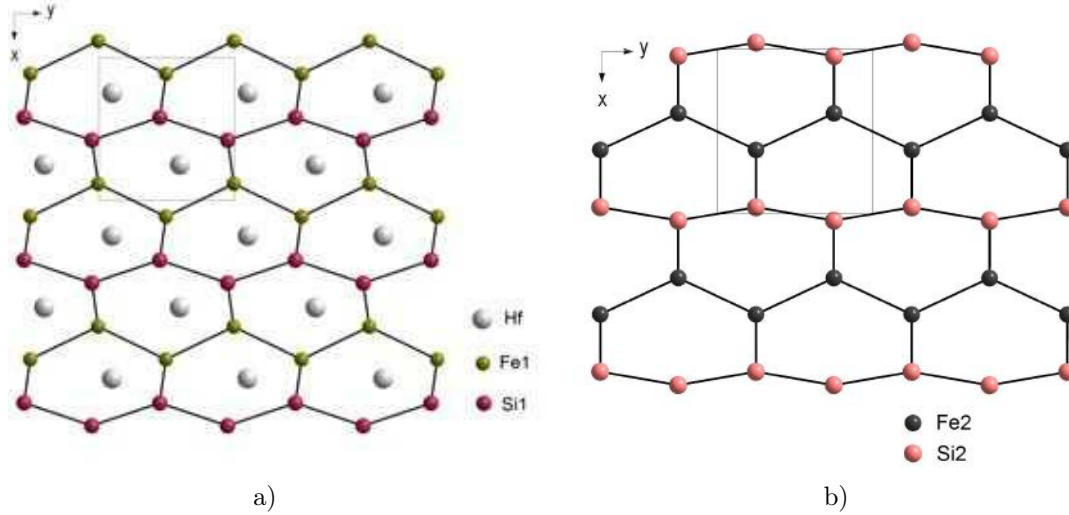


Fig. 2. Flat Hf-centered distorted hexagonal nets formed by the Fe1 and Si1 atoms at  $z = \frac{1}{4}, \frac{3}{4}$  (a), and distorted hexagonal nets formed by the Fe2 and Si2 atoms at  $z = 0, \frac{1}{2}$  (b).

It is still not well understood why among more than 300  $RM_2X_2$  ternary intermetallic compounds, where  $M$  is a transition  $d$ -element and  $X$  is an  $sp$ -element (P, Al, Si, Ga, Ge), just two compounds  $\text{ScFe}_2\text{Si}_2$  and  $\text{HfFe}_2\text{Si}_2$  have a distinctive and unique crystal lattice, in which Fe and Si occupy two non-equivalent crystallographic positions. To reveal the electronic structure as well as the type of chemical bonds in this particular family of intermetallic compounds, we have conducted systematic X-ray spectroscopic investigations of  $\text{HfFe}_2\text{Si}_2$ . Also, we have calculated the X-ray emission spectra for this compound from first principles and compared the obtained results with experiment.

## II. DETAILS OF EXPERIMENT AND THEORETICAL CALCULATIONS

The samples of the  $\text{HfFe}_2\text{Si}_2$  alloy were prepared by arc melting of pure constituent elements on a water-cooled copper hearth under pure argon atmosphere. The homogenization of the samples was conducted under vacuum at  $800^\circ\text{C}$  during 350 h in sealed quartz ampoules as was described in Ref. [1]. The phase composition of the samples was analyzed using X-ray diffraction technique (a DRON-2 diffractometer,  $\text{FeK}_\alpha$ -radiation).

Space group	Lattice parameters, nm			Lattice ratios	
	$a$	$b$	$c$	$b/a$	$c/a$
Pbcm	0.7445(5)	0.7054(5)	0.5057(3)	0.94748	0.67925

Table 1. The structural characteristics of  $\text{HfFe}_2\text{Si}_2$ .

Atom	$x/a$	$y/b$	$z/c$
Hf	0.2489	0.0957	0.25
Fe1	0.1147	0.4930	0.25
Fe2	0.6111	0.25	0
Si1	0.4201	0.4477	0.25
Si2	0.9595	0.25	0

Table 2. The atomic coordinates in  $\text{HfFe}_2\text{Si}_2$  [1].

Distance	nm	Distance	nm
Si-Si	0.2890 (Si1-Si1)	Fe-Fe	0.2529 (Fe2-Fe2)
	0.2529 (Si2-Si2)		
Si-Fe	0.2278 (Si2-Fe1)	Hf-Si	0.2676 (Hf-Si1)
	0.2296 (Si1-Fe1)		0.2725 (Hf-Si2)
	0.2359 (Si1-Fe2)		0.2791 (Hf-Si1)
	0.2423 (Si2-Fe1)	Hf-Fe	0.2848 (Hf-Si1)
	0.2490 (Si1-Fe2)		0.2790 (Hf-Fe1)
	0.2594 (Si2-Fe2)		0.2802 (Hf-Fe1)
			0.2938 (Hf-Fe2)

Table 3. The nearest-neighbor distances in the HfFe<sub>2</sub>Si<sub>2</sub> structure. Radius of atoms: Hf — 0.1564 nm, Fe — 0.126 nm, Si — 0.117 nm [6].

The obtained X-ray powder diffraction data were analyzed by CSD software [5] developed at the Ivan Franko National University of Lviv. The interatomic distances in the HfFe<sub>2</sub>Si<sub>2</sub> structure were calculated using the atomic coordinates published in Ref. [1] (see Table 1 and Table 2). The resulting parameters (Table 3) agree well with available data [1].

The experimental setup for Fe and Si *K*- and *L*- X-ray emission spectra measurements was described earlier in Ref. [7].

The calculations of electron energy bands  $E(k)$ , partial DOS (density of states) and X-ray emission spectra for HfFe<sub>2</sub>Si<sub>2</sub> were performed by the semi-relativistic LMTO (linear muffin-tin orbital) method without taking into consideration the spin-orbit interaction. The exchange potential in the form of Barth and Hedin was used [8]. The eigenvalues were calculated at 252 points within a 1/16 of the Brillouin zone.

### III. RESULTS AND DISCUSSION

As we noticed above, the investigated structure differs from the known CeGa<sub>2</sub>Al<sub>2</sub> structural type, since iron and silicon occupy two non-equivalent crystallographic positions labeled in Fig. 1 and Fig. 2 as Fe1, Fe2 and Si1, Si2, respectively. In such a case, due to insufficient resolution, the experimental X-ray emission spectrum frequently does not allow accurate determination of the contributions of each atom to the total density of states. We used the LMTO method to calculate total and partial electron densities of states, as well as to evaluate separately X-ray emission spectra for the crystallographically non-equivalent iron and silicon atoms.

As emission spectra of Hf have an extremely low intensity, they can be obtained only with enormous efforts by a long-time exposition. Because of high excitation energy of the *K* level of hafnium and its significant width, and hence its low informativeness, the *K* emission spectrum of hafnium is not useful.

The obtained theoretical and experimental X-ray emission spectra of Hf, Fe and Si are shown in Figs. 3–7. Good agreement between the experimental and theoret-

ical curves is observed for the *K* and *L* bands of Fe. In general, the presence of the Fe*K* $\beta''$ -satellite indicates  $4p \rightarrow 1s$  transitions as a feature of the Fe*K* $\beta_{2,5}$ -band. The main maximum *C* (Fig. 3) of the Si*L*<sub>II,III</sub>-band ( $3s \rightarrow 2p$  transitions) coincides in energy with the maximum *F* (the Fe*K* $\beta''$ -satellite) and indicates a considerable contribution of the hybridized Si *s*-states to the intensity of the Fe*K* $\beta_{2,5}$ -band (Fig. 5).

The experimental Si *K* $\beta$ -band ( $3p \rightarrow 1s$  transitions) turns out to be wider than the theoretical one. The Si*L*-spectra mainly reflect the distribution of *s*-states. The band *A* in the Si*L*-emission energetically coincides with the main maximum in Fe*L*-emission (Fig. 6), which indicates strong hybridization between the iron *d*-states and silicon *s*-states in the energy range between 0 and 5 eV. The degree of hybridization substantially depends on the nearest neighbors of silicon. The maximum near the Fermi level is typical of binary and ternary compounds [9–13]. The calculated intensity of the X-ray emission from Si2 (Fig. 3) is lower than for Si1. It is consistent with the crystal structure analysis that shows that the atomic Fe1–Si distances are significantly smaller than the ones in the polyhedrons containing Fe2 (Table 3).

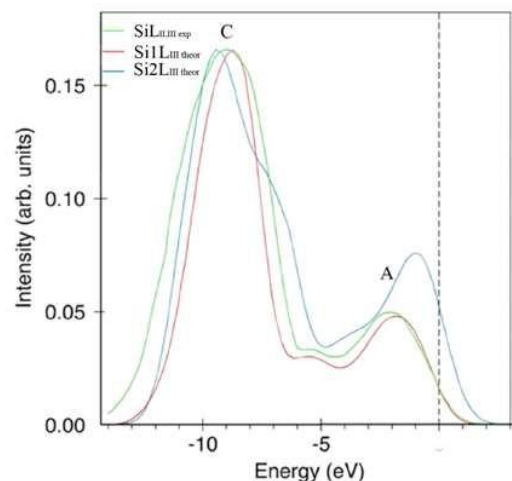


Fig. 3. Calculated and experimental X-ray emission Si *L*<sub>2,3</sub>-bands in HfFe<sub>2</sub>Si<sub>2</sub>.

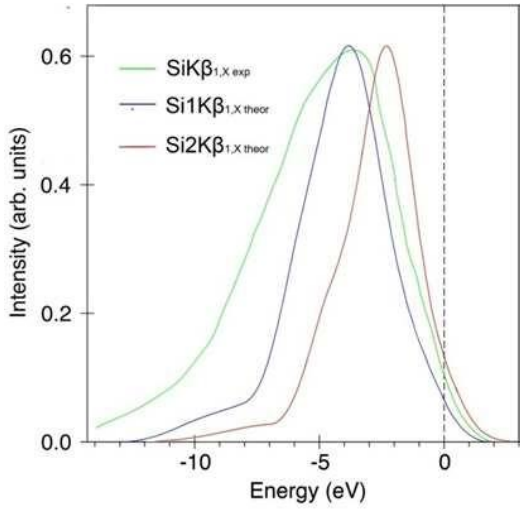


Fig. 4. Calculated and experimental X-ray emission  $\text{Si}K\beta_{1,x}$ -bands in  $\text{HfFe}_2\text{Si}_2$ .

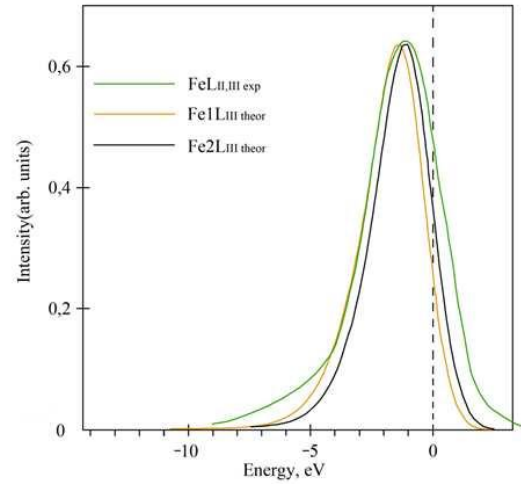


Fig. 6. Calculated and experimental X-ray emission  $\text{Fe}L_{\text{II,III}}$ -bands in  $\text{HfFe}_2\text{Si}_2$ .

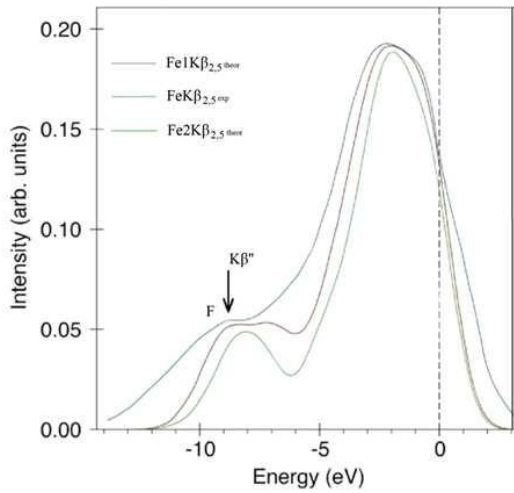


Fig. 5. Calculated and experimental X-ray emission  $\text{Fe}K\beta_{2,5}$ -bands in  $\text{HfFe}_2\text{Si}_2$ .

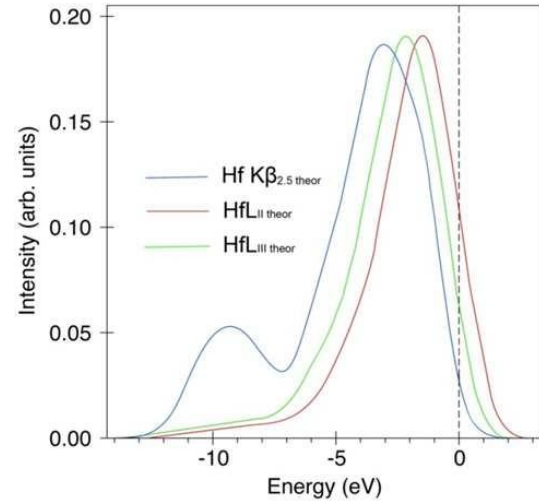


Fig. 7. Calculated X-ray emission  $\text{Hf}K\beta_{2,5}$ - and  $\text{Hf}L_{\text{II,III}}$ -bands in  $\text{HfFe}_2\text{Si}_2$ .

Component	$K$ -band		$L_{\text{II}}$ -band		$L_{\text{III}}$ -band		
	$p_{1/2}$	$p_{3/2}$	$s_{1/2}$	$d_{3/2}$	$s_{1/2}$	$d_{3/2}$	$d_{5/2}$
Hf	32.46	67.54	5.17	94.83	5.35	9.54	85.11
Fe1	32.16	67.84	0.42	99.58	0.45	10.16	89.39
Fe2	32.18	67.82	0.45	99.55	0.48	10.17	89.36
Si1	33.18	66.82	76.13	23.87	80.27	3.02	16.71
Si2	33.26	66.74	80.32	19.68	81.36	2.07	16.57

Table 4. Calculated contributions of different electronic states to the intensity of X-ray emission bands of  $\text{HfFe}_2\text{Si}_2$  (in %).

A similar trend is observed for the Si X-ray emission spectra in the 6–11 eV energy range, which reflects covalent Si–Si bonds. Indeed, according to Table 3, the Si1–Si1 distance (0.2890 nm) is much larger than Si2–Si2 (0.2529 nm), which correlates well with the calculated emission intensities from Si1 and Si2.

Fig. 5 shows the experimental and theoretically calculated  $\text{Fe}K\beta_{2,5}$ -bands, which reflect, according to the selection rules, the density distribution of the filled Fe valence  $p$ -states. A nearly total coincidence is observed for the maxima positions of all three curves. At the same time, we should distinguish the anomalous  $\text{Fe}K\beta_{2,5}$ -band

splitting of the Fe2 band. Due to the considerable diffusivity of the Fe $p$ -wave functions, the full width at half maximum of the experimental spectrum is larger than that of the theoretical curves.

The X-ray emission  $L$ -band of transition elements makes it possible to obtain the information about the distribution of  $d$ -symmetry electrons (Fig. 6). As can be concluded from Table 4, the main contribution to the calculated intensity of  $L_{II,III}$ -band of iron in two crystallographically non-equivalent positions is indeed from the electron states of  $d$ -symmetry.

The ratio of the contributions from  $d_{3/2}$ - and  $d_{5/2}$ -

states to the emission band intensity is considered to be one of the most important characteristics of the spin-orbit interaction in the valence band. Without taking into account the spin-orbit interaction, this ratio is:

$$\frac{I_{d_{5/2}}}{I_{d_{3/2}}} = 9. \quad (1)$$

As can be seen from Table 4, this ratio calculated for the  $L_{III}$ -valence band does not differ considerably from the above number. This indicates that the spin-orbit interaction is small and can be neglected.

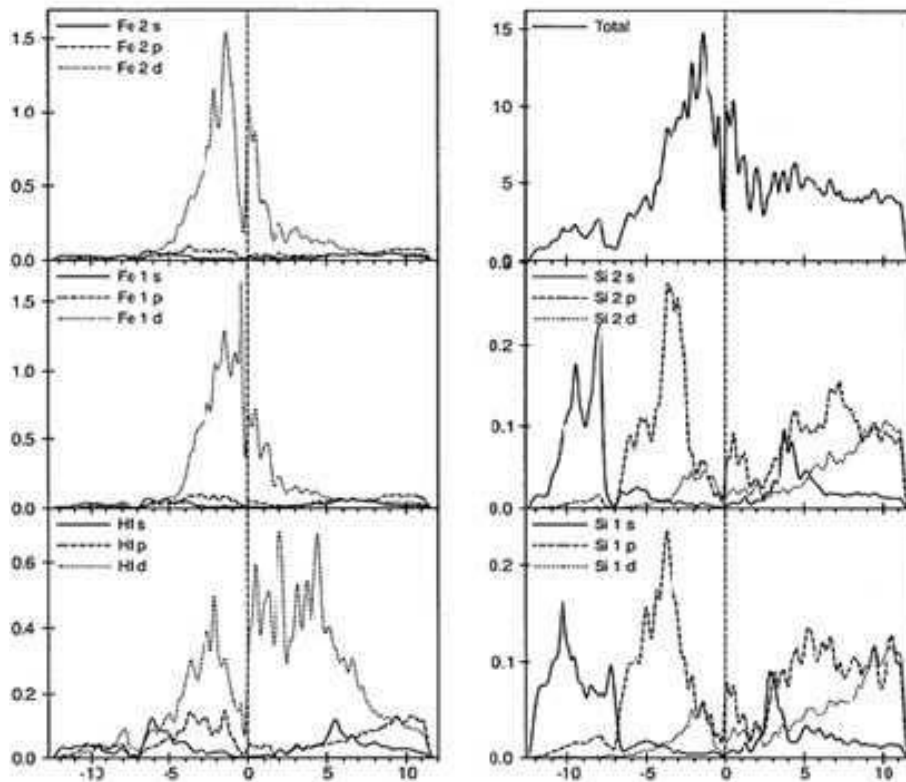


Fig. 8. Total and partial densities of electronic states in HfFe<sub>2</sub>Si<sub>2</sub>.

The total and partial densities of states for HfFe<sub>2</sub>Si<sub>2</sub> are shown in Fig. 8. The effective numbers of valence electrons of different symmetries per atom  $N_{\chi}$  can be estimated from the partial density of electron states as follows:

$$N_{\chi} = \int_{E_0}^{E_F} N_{\chi}(E) dE, \quad (2)$$

where  $N_{\chi}(E)$  is the partial DOS which corresponds to the relativistic quantum number  $\chi$ ,  $E_0$  is the energy of the bottom of the valence band,  $E_F$  is the Fermi energy. The results of such estimation for HfFe<sub>2</sub>Si<sub>2</sub> are shown in Table 5. The analysis of the results shows that the degree of the occupation of  $spd$ -valence orbitals varies and con-

siderably differs from the number of external electrons in isolated atoms.

Atom	$s$	$p$	$d$
Hf	0.80109	1.26794	3.14885
Fe1	0.61610	0.90307	6.93593
Fe2	0.58230	0.85550	6.88833
Si1	1.04750	1.54706	0.27180
Si2	1.05851	1.52757	0.26072

Table 5. Effective filling numbers of valence band electrons of different symmetries in HfFe<sub>2</sub>Si<sub>2</sub>.

The occupancy of the  $d$ -orbital of Hf in HfFe<sub>2</sub>Si<sub>2</sub> is significantly larger than that in an isolated state. In our

opinion, the most interesting is the analysis of the change of external valence  $sp$ -states occupation, as it gives the possibility to estimate the contribution of Si electrons to the chemical bond of  $\text{HfFe}_2\text{Si}_2$ . The electron configuration of Si in the compound can be described as  $s^{1.1}p^{1.5}$  (Table 5), which significantly differs from  $s^2p^2$  (atomic Si). Thus, we can conclude that in the investigated compound the Si atoms contribute 0.9 electrons of  $s$ -symmetry per atom to the chemical bond (for comparison, the Si atoms contribute 0.7 electrons per atom in  $\text{YM}_2\text{Si}_2$  compounds [12]). A similar situation was also observed in the case of  $\text{CeM}_2\text{P}_2$  compounds [7]. It is important to note that the contribution of the  $s$ -symmetry electrons to the chemical bond is substantially different for Si1 and Si2.

Due to the fact that the investigated  $\text{HfFe}_2\text{Si}_2$  compound is a ferromagnetic material with high Curie temperature ( $T_c = 900$  K) and at the same time manifests

semiconductor-type resistivity temperature dependence  $\rho(T)$ , it would be reasonable to explore the magnetic state of its iron atoms.

## CONCLUSIONS

As can be seen from the obtained theoretical and experimental data, in  $\text{HfFe}_2\text{Si}_2$  the  $s$ -states of Si hybridize with the  $p$ -states of Si and Fe and are located at the bottom of the valence band. In the middle of the valence band, the  $p$ -states of the constituent atoms are localized, whereas near the Fermi level the Fe  $d$ -states dominate. The contribution of the  $s$ -symmetry electrons to the chemical bond is substantially different for the Si atoms located in non-equivalent crystallographic positions.

- 
- [1] Ya. P. Yarmolyuk, L. A. Lysenko, E. I. Gladyshevskiy, *Sov. Phys. Crystallogr.* **21**, 473 (1976).  
 [2] E. I. Gladyshevskiy, O. I. Bodak, *Crystal Structure of the Rare Earth Intermetallic Compounds* (Vyshcha Shkola, Lviv, 1982) [in Russian].  
 [3] Z. Ban, M. Sikirica, *Acta Crystallogr.* **18**, 594 (1965).  
 [4] E. I. Gladyshevskiy, B. Ja. Kotur, O. I. Bodak, V. P. Skvorchuk, *Dop. Akad. Nauk URSR A* **8**, 751 (1977) [in Ukrainian].  
 [5] L. Akselrud, Yu. Grin, *J. Appl. Crystallogr.* **47**, 803 (2014); <https://doi.org/10.1107/S1600576714001058>.  
 [6] N. Wiberg, *Lehrbuch der Anorganischen Chemie* (Walter de Gruyter, Berlin, 1995), p. 1838.  
 [7] I. D. Shcherba *et al.*, *J. Electron. Spectrosc. Relat. Phenom.* **131–132**, 125 (2003); [https://doi.org/10.1016/S0368-2048\(03\)00127-0](https://doi.org/10.1016/S0368-2048(03)00127-0).  
 [8] U. Von Barth, L. Hedin, *J. Phys. C* **5**, 1629 (1972); <https://doi.org/10.1088/0022-3719/5/13/012>.  
 [9] P. J. W. Weijs *et al.*, *Z. Phys. B Condens. Matter* **78**, 423 (1990); <https://doi.org/10.1007/BF01313324>.  
 [10] P. J. W. Weijs *et al.*, *Phys. Rev. B* **44**, 8195 (1991); <https://doi.org/10.1103/PhysRevB.44.8195>.  
 [11] I. Jarrige, N. Capron, P. Jonnard, *Phys. Rev B* **79**, 035117 (2009); <https://doi.org/10.1103/PhysRevB.79.035117>.  
 [12] I. D. Shcherba, V. N. Antonov, B. Y. Kotur, *J. Alloys Comp.* **242**, 58 (1996); [https://doi.org/10.1016/0925-8388\(96\)02335-3](https://doi.org/10.1016/0925-8388(96)02335-3).  
 [13] I. D. Shcherba *et al.*, *J. Electron Spectrosc. Rel. Phenom.* **212**, 5 (2016); <https://doi.org/10.1016/j.elspec.2016.07.0020>.

## ЕЛЕКТРОННА СТРУКТУРА ТА Х-ПРОМЕНЕВІ СПЕКТРОСКОПІЧНІ ОСОБЛИВОСТІ СПОЛУКИ $\text{HfFe}_2\text{Si}_2$

І. Д. Щербач<sup>1</sup>, В. М. Антонов<sup>2</sup>, О. В. Жак<sup>1</sup>, Л. В. Бекенов<sup>2</sup>, М. В. Ковальська<sup>1</sup>,  
 Н. Нога<sup>3</sup>, Д. Узкокович<sup>4</sup>, Б. М. Яцик<sup>5</sup>

<sup>1</sup>Львівський національний університет імені Івана Франка,  
 вул. Кирила і Мефодія, 6/8, 79005, Львів, Україна

<sup>2</sup>Інститут металофізики НАН України, вул. Вернадського, 36, 03142, Київ, Україна

<sup>3</sup>Інститут техніки, Педагогічний університет, вул. Подхоронжих, 2, 30084, Краків, Польща

<sup>4</sup>Інститут техніки, САНУ, Белград, Сербія

<sup>5</sup>Львівський національний університет ветеринарної медицини і біотехнології, Львів, Україна

Методом Х-променевої спектроскопії вперше досліджено електронну структуру валентної зони сполуки  $\text{HfFe}_2\text{Si}_2$ . Унікальність цієї сполуки полягає в тому, що вона разом з інтерметалідом  $\text{ScFe}_2\text{Si}_2$  має кристалічну структуру, відмінну від широко розповсюдженого типу  $\text{CeGa}_2\text{Al}_2$ .

Для сполуки  $\text{HfFe}_2\text{Si}_2$  методом ЛМТО з метою одержання розподілу інтенсивностей у рентгенівських емісійних спектрах ми вперше розрахували повну та парціальну густини електронних станів гафнію, заліза та кремнію. Розрахунок здійснено у 209-х точках 1/16 зони Бріллюена в напіврелятивістському наближенні. Обмінний потенціал вибирали в наближенні Барта–Гедіна. Зіставлення розрахованих та експериментально одержаних рентгенівських смуг для більшості випадків ілюструє задовільне узгодження. Дослідженій сполуці притаманно те, що залізо і кремній мають по дві кристалічно нееквівалентні позиції. Як відомо, рентгенівські експериментальні спектри не дають змоги розділити внески в загальну густину станів від кожної

з компонент. Це можна зробити лише теоретичними розрахунками. У роботі представлено суміщені в єдиній енергетичній шкалі спектри заліза і кремнію. Високоенергетична частина спектра кремнію відображає *d*-густину станів заліза, які проявляються у спектрі внаслідок гібридизації з *s*-станами кремнію.

Ступінь гібридизації істотно залежить від найближчого оточення кремнію, і в Si2 інтенсивність цього максимуму є значно нижчою, ніж у Si1. Установлено, що дно валентної зони сформовано *s*-станами кремнію, які гібридизуються з *p*-станами заліза. На відміну від електронної конфігурації кремнію в елементарному стані ( $s^2p^2$ ) та в кристалічному стані ( $s^1p^3$ ), у сполуці HfFe<sub>2</sub>Si<sub>2</sub> становить ( $s^{1.1}p^{1.5}$ ).